

Dielectric Properties of Potassium Doped Sodium Tantalate Ceramic

V. Lingwal¹, A. S. Kandari², N. S. Panwar³

¹ Department of Physics, Pt. L.M.S. Government PG College Rishikesh, Dehradun, India

² Department of Physics, Government PG College New Tehri, India

³ University Science Instrumentation Center, HNB Garhwal University, Srinagar (Garhwal), India

Abstract: Pellet samples of sodium-potassium tantalate ($\text{Na}_{1-x}\text{K}_x\text{TaO}_3$) mixed system (for $x = 0, 0.2, 0.4, 0.5, 1$) compositions were prepared using solid state reaction method. Samples were prepared by pressing the calcined mixture at 0.2 MPa and sintered in a tube furnace opened at both ends. Prepared samples were characterized by x-ray diffraction (XRD) and energy dispersive x-ray analysis (EDAX) method. In the XRD patterns, shifting of most intense peaks, to lower angle was observed with increasing x value in the prepared compositions; except for $x = 0.5$, where a break in the peak shifting pattern was observed. Lattice parameters and crystallite size for different compositions were calculated from the XRD data. EDAX results show marked sodium escaping from the prepared samples. Frequency and x dependence of dielectric constant, loss tangent and dielectric conductivity have been studied in the frequency range from 0.01 MHz to 10 MHz, at room temperature. With increasing frequency dielectric constant and loss tangent were found decreasing, which indicate relaxational behaviour of this system. Dielectric constant was observed decreased for the compositions with $x = 0.2$ and 0.5 with respect to their nearby x , showing morphotropic phase transitions in these regions; however, loss tangent and dielectric conductivity were observed decreased only for $x = 0.5$ composition.

Keywords: Ferroelectrics, perovskite, dielectric constant, loss tangent, sintering.

I. INTRODUCTION

The perovskite (ABO_3) type alkali metal niobates and tantalates constitute an important group of oxide compounds with broad range of technologically important dielectric, piezoelectric, ferroelectric and optoelectronic properties [1]. Among these compounds sodium potassium niobate ($\text{Na}_{1-x}\text{K}_x\text{NbO}_3$) and sodium potassium tantalite ($\text{Na}_{1-x}\text{K}_x\text{TaO}_3$) have attracted considerable attention. Solid solutions can be formed over the whole composition range ($x = 0$ to 1), allowing a high degree of tailorability of physical properties for these mixed oxides. For low x values these systems appear to exhibit true phase transitions and the dielectric properties can be understood in terms of soft optic phonons [2, 3].

Interest has centered on $\text{Na}_{1-x}\text{K}_x\text{TaO}_3$ system, especially in relation to quantum effects, suppression of the phase transition and the question of long-range order vs glasslike behavior [4]. $\text{Na}_{1-x}\text{K}_x\text{TaO}_3$ system has interesting end

members, i.e., NaTaO_3 is ferroelectric and KTaO_3 is paraelectric, at room temperature [5]. Davis [3] has observed that, for $x \geq 0.70$, this system shows a single phase transition from the high temperature cubic paraelectric phase to a tetragonal ferroelectric phase (CT). For $0.70 \geq x \geq 0.45$, it shows two ferroelectric transitions, a cubic to tetragonal transition followed by a lower temperature transition to a phase believed to have an orthorhombic symmetry [3]. Samara [1] has found the pressure dependence of CT transition, in $\text{Na}_{0.28}\text{K}_{0.72}\text{TaO}_3$ single crystal, consistent with the soft mode theory.

$\text{Na}_{1-x}\text{K}_x\text{TaO}_3$ is a comparatively less studied system. Investigators have studied the low temperature dielectric behavior of $\text{Na}_{1-x}\text{K}_x\text{TaO}_3$ single crystals [1, 3]. In the present study observations on dielectric properties of the mixed $\text{Na}_{1-x}\text{K}_x\text{TaO}_3$ system for different compositions ($x = 0, 0.2, 0.4, 0.5, 1$), at room temperature, were carried out.

II. PREPARATION

In the present study samples were prepared with conventional solid-state reaction method. The starting materials, used for preparing $\text{Na}_{1-x}\text{K}_x\text{TaO}_3$ system, were sodium carbonate (Na_2CO_3), potassium carbonate (K_2CO_3) and tantalum pentoxide (Ta_2O_5). The purity of all the starting materials was 99.95%. The starting materials were initially dried, at 150 °C, to remove the absorbed moisture. K_2CO_3 is a hygroscopic material and hence due care was taken in its handling. Different compositions of $\text{Na}_{1-x}\text{K}_x\text{TaO}_3$ ($x = 0, 0.2, 0.4, 0.5, 1$) were prepared by weighing the starting materials in stoichiometric ratio. Each composition was manually dry mixed for 1 hour and with methyl alcohol for another 1 hour using agate mullet mortar and pestle. The mixture was calcined in an alumina crucible, in ambient atmosphere, at 950 °C for 2 hours, to remove carbonates present in the mixture. After cooling, in dry air, the calcined mixture was weighed to ensure complete carbonate removal from the mixture. Calcined mixture was pressed at 0.2 MPa to form the pellets of 6 mm diameter. These raw pellets were sintered in a tube furnace opened at both ends. All the pellet samples, except NaTaO_3 , were placed in an alumina crucible and sintered at 1050 °C, for 15 hours. NaTaO_3 pellets were sintered at 1100 °C for 15 hours, due to their high melting

point. All the samples were taken out from the furnace when it cooled to room temperature. Sintered pellets were electroded, with air-drying silver paste, in metal-insulator-metal (MIM) configuration for dielectric measurements.

III. CHARACTERIZATION

Room temperature x-ray diffraction (XRD) patterns of all the pellet samples were taken by Philips Analytical X-ray Diffractometer (PW3710), using $\text{CuK}_{\alpha 1}$ radiation of wavelength 1.54056\AA . Peak indexing was done by using Joint Committee on Powder Diffraction Standards data cards. Crystallite size of the samples was calculated from the full width at half maximum (FWHM) of the highest intensity peak in the XRD pattern [6], and the perovskite subcell parameters were obtained using the relation provided by Azaroff [7]. Fig. 1 shows the observed XRD patterns of $\text{Na}_{1-x}\text{K}_x\text{TaO}_3$ system. The diffraction peaks were observed shifting towards lower angle with increasing x value; except for x = 0.5, where a break in the pattern of peak shifting is observed.

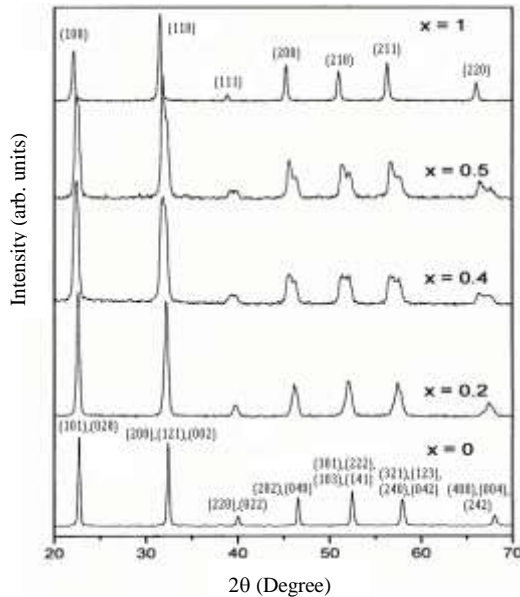


Fig.1 X-ray diffraction patterns of $\text{Na}_{1-x}\text{K}_x\text{TaO}_3$ samples, at room temperature.

The observed positions of most intense diffraction peaks for different compositions (x values) have been given in Table 1.

Table – 1

Positions of most intense x-ray diffraction peaks of $\text{Na}_{1-x}\text{K}_x\text{TaO}_3$ for different x values

x	Peaks (101),(020) (200), (121), (002)	
	2θ (in degree)	
0	22.705	32.395
0.2	22.600	32.120
0.4	22.415	31.605

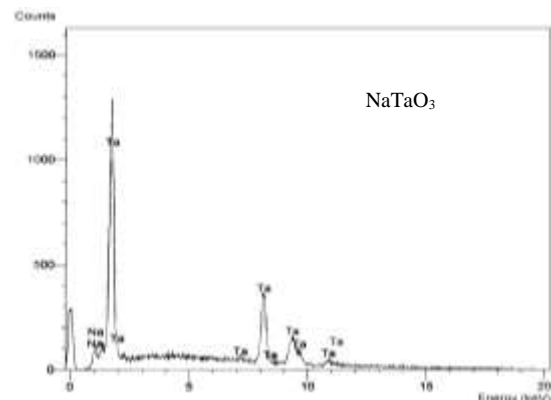
0.5	22.645	31.755
1	22.150	31.495

Also the patterns, corresponding to x = 0 and x = 1, altogether show different indexing, indicating transformation to a new material. Using the observed XRD data, the calculated lattice parameters for NaTaO_3 were obtained as $a = 5.5228\text{\AA}$, $b = 7.7847\text{\AA}$ and $c = 5.5451\text{\AA}$; and for KTaO_3 these were obtained as $a = 4.0199\text{\AA}$, $b = 4.0201\text{\AA}$ and $c = 4.0195\text{\AA}$. The calculated lattice parameter values were found comparable to the reported values [8, 9]. The crystallite sizes calculate from the XRD data of the prepared samples have been given in Table 2. Addition of potassium, generally, shows a decrease in the crystallite size in this system. All potassium-incorporated samples were sintered at same temperature, at 1050°C , in the present study. However, it is worth noting that the melting points of this material decrease with increasing potassium content [10], and hence ideally the sintering temperature of these samples should be varied accordingly. The observed decrease in crystallite size with increasing x values, in these samples, may be due to their sintering at the same temperature.

Table – 2
Crystallite size of $\text{Na}_{1-x}\text{K}_x\text{TaO}_3$ for different x values

Composition ($\text{Na}_{1-x}\text{K}_x\text{TaO}_3$)	x = 0	x = 0.2	x = 0.4	x = 0.5	x = 1
Crystallite Size (μm)	0.0338	0.0219	0.0130	0.0108	0.0237

Chemical analysis of the prepared samples was done by Jeol Scanning Microscope (JSM-840) using energy dispersive x-ray analysis (EDAX). The observed EDAX results of this system have been shown in Fig. 2. The observed and calculated EDAX results have been given in Table 3, for the present samples. The observed weight percentage of Na was found less than the calculated values, which indicates that sodium escapes from the lattice of these samples. However, significant escaping of potassium was not observed.



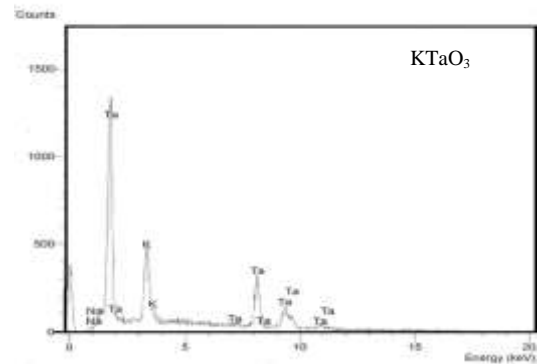
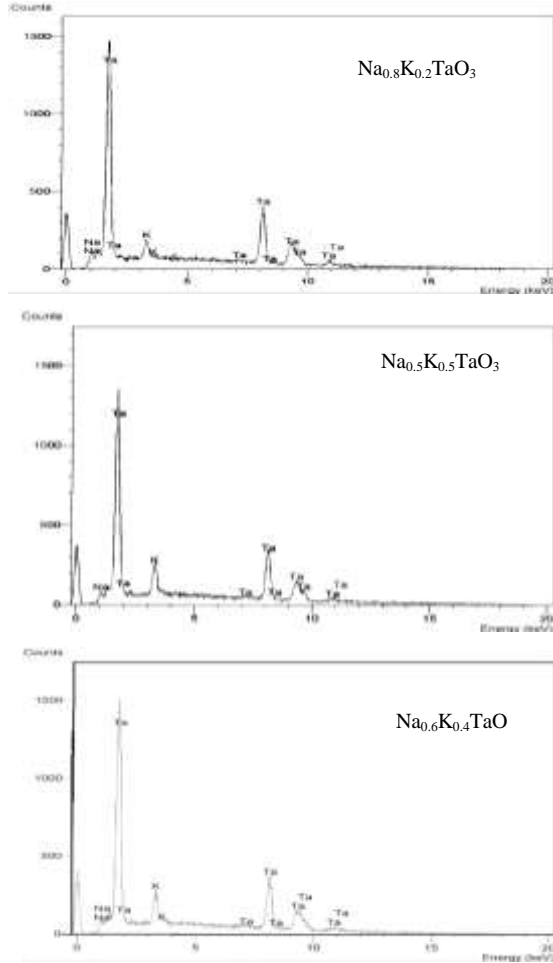


Fig. 2. EDAX results of Na_{1-x}K_xTaO₃ system for different x values.

IV. DIELECTRIC MEASUREMENTS

Dielectric properties of Na_{1-x}K_xTaO₃ ceramics vary with x and preparation conditions. Frequency (from 0.01 MHz to 10 MHz) dependence of dielectric properties of Na_{1-x}K_xTaO₃ system, for different x values has been investigated, in the present study. At room temperature, decrease in the dielectric properties at a particular concentration (x value), relaxation behavior, and break in the peak shifting in the XRD patterns were observed in this system.

For studying the frequency and concentration dependence of dielectric properties measurements were made, run to run on the same sample and sample to sample for all samples prepared with the similar method, in the frequency range from 0.01 MHz to 10 MHz, at room temperature. The observations

Table – 3
 Energy dispersive x-ray analysis (EDAX) results of Na_{1-x}K_xTaO₃ system

Materials	Weight % (calculated)			Weight % (observed)			Atomic % (calculated)			Atomic % (observed)		
	Na	K	Ta	Na	K	Ta	Na	K	Ta	Na	K	Ta
NaTaO ₃	11.3	--	88.7	6.9	--	93.1	49.0	--	51.0	37.0	--	63.0
Na _{0.8} K _{0.2} TaO ₃	8.9	3.8	87.3	4.6	4.5	90.9	40.4	9.6	50.0	24.6	13.6	61.8
Na _{0.6} K _{0.4} TaO ₃	6.6	7.4	86.0	3.8	7.4	88.8	30.0	20.0	50.0	19.5	22.5	58.0
Na _{0.5} K _{0.5} TaO ₃	5.4	9.2	85.4	3.7	8.6	87.7	25.0	25.0	50.0	18.6	25.6	55.8
KTaO ₃	--	17.7	82.3	--	17.2	82.8	--	50.0	50.0	--	49.0	51.0

were close to each other and the values were averaged. Capacitance and dissipation factor measurements were carried out in MIM configuration, using Fluke – PM6306 RCL meter and HP- 4275 Multifrequency LCR meter. Dielectric constant (K) was calculated by the relation,

$$K = C/C_0,$$

where C and C₀ are the capacitances of the electrodes with and without dielectric, respectively; C₀ is given by,

$$C_0 = (0.0885 \pi r^2/d) \text{ pF},$$

where r (cm) is the radius of the electrodes and d (cm) distance between them.

Dielectric conductivity (σ) was calculated by the relation,

$$\sigma = \epsilon_0 \omega K \tan \delta,$$

where ϵ_0 is the permittivity of free space, $\tan \delta$ the dissipation factor, and $\omega = 2 \pi f$, f the applied frequency.

V. RESULTS AND DISCUSSION

Observed frequency dependence of dielectric constant and dielectric loss, for different x values, in $\text{Na}_{1-x}\text{K}_x\text{TaO}_3$ samples has been shown in Figs. 3 and 4. Dielectric constant and loss tangent decrease with increasing frequency, and at higher frequencies dielectric constant remains constant, at room temperature. Variation of the dielectric constant with composition (x) is shown in Fig. 5. Dielectric constant was observed decreased at $x = 0.2$ and 0.5 (with respect to other nearby compositions, x) for all the measured frequencies. Dielectric loss increases with increasing x value, for $x \leq 0.4$; however, for $x = 0.5$, it decreases, and further increases for

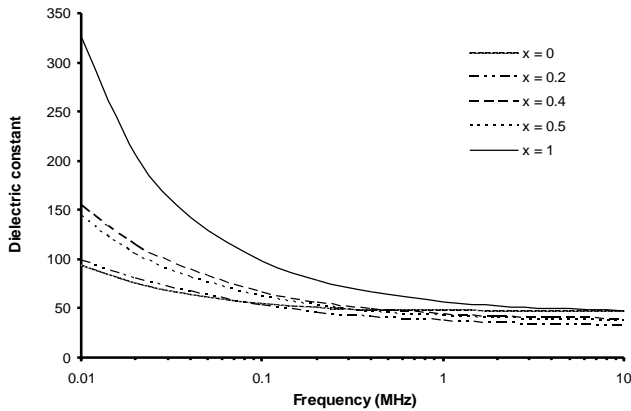


Fig. 3. Frequency dependence of dielectric constant of $\text{Na}_{1-x}\text{K}_x\text{TaO}_3$, for different x values, at room temperature.

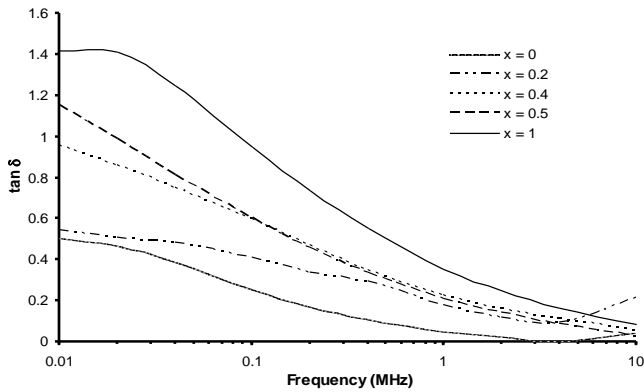


Fig. 4. Frequency dependence of loss tangent ($\tan \delta$) of $\text{Na}_{1-x}\text{K}_x\text{TaO}_3$, for different x values, at room temperature.

$x = 1$, Fig. 6.

Decreasing nature of dielectric constant with increasing frequency may be due to the relaxational behavior of a material [11]. Lossy dielectrics can be represented by the circuit analog of a resistance in parallel with a capacitor [11]. At higher frequency the capacitor offers low reactance to the sinusoidal signal, which minimizes the conduction losses in the resistor. Hence, the value of dielectric loss decreases with increasing frequency.

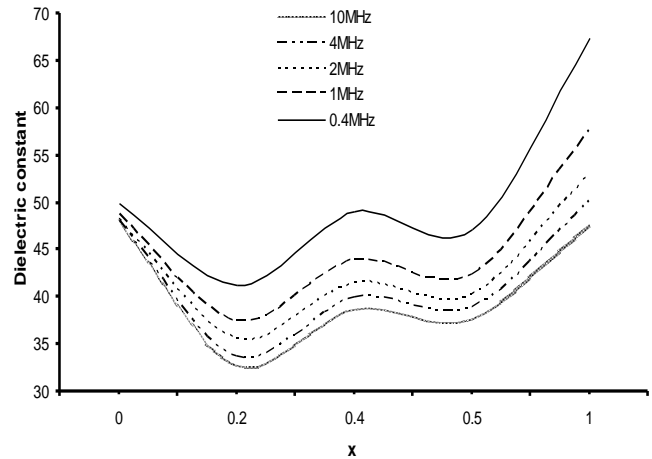


Fig. 5. x dependence of dielectric constant in $\text{Na}_{1-x}\text{K}_x\text{TaO}_3$, for different frequencies, at room temperature.

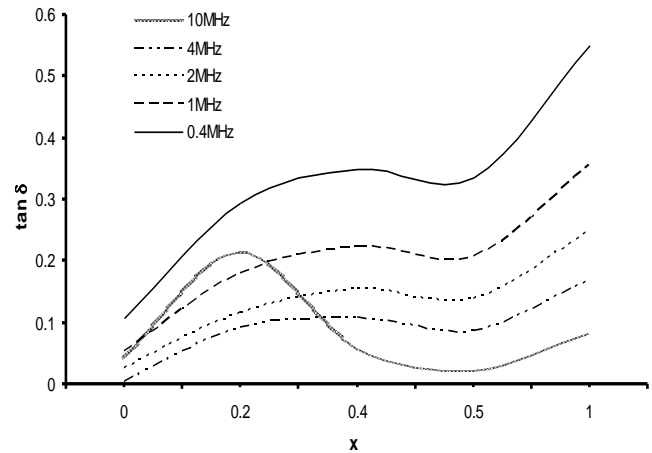


Fig. 6. x dependence of dielectric loss ($\tan \delta$) in $\text{Na}_{1-x}\text{K}_x\text{TaO}_3$, for different frequencies, at room temperature.

The observed x dependence of dielectric conductivity (σ), of the prepared samples of $\text{Na}_{1-x}\text{K}_x\text{TaO}_3$, is shown in Fig. 7, for different frequencies, at room temperature. Dielectric conductivity increases with increasing x values; except for $x = 0.5$, where it was found decreased. Dielectric conductivity (σ) was observed, generally, increasing with increasing frequency.

In an ac field, electrical conductivity and dielectric constant are related by dissipation factor, which measures the energy loss per cycle (usually in the form of heat) from the material. For $x = 0.5$ composition the conductivity decreases. This behaviour seems interesting in the composition-property diagram of solid solution. It shows some transition in a solid solution on change in composition.

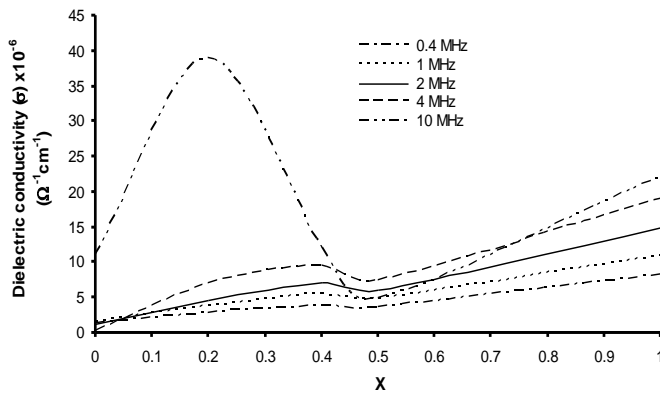


Fig. 7. x dependence of dielectric conductivity in $\text{Na}_{1-x}\text{K}_x\text{TaO}_3$, for different frequencies, at room temperature.

For solid solution of $\text{Na}_{1-x}\text{K}_x\text{TaO}_3$, the concentration dependence of σ exhibits minima, the position of which closely agrees with the results of dielectric constant and loss tangent measurements, and break in tendency of peak shifting in the XRD pattern.

The principle types of intrinsic defects, in ABO_3 compounds, are vacancies at the A [V_A] and oxygen [V_O] site [12]. During sintering the intensification of diffusion processes in specimens, enhances the possibility of escape of the highly volatile alkali metal ions from the lattice. The V_A concentration in such specimens is higher than in specimens of different composition, n-type conductivity is more probable in pure NaNbO_3 and NaTaO_3 [13, 14] but it may be very unstable. It seems that the same is true for $\text{Na}_{1-x}\text{K}_x\text{TaO}_3$ for different x values. This assumption seems reasonable, because in this system there is only isovalent substitution of ions; this promotes a decrease in the number of lattice vacancies [12]. With this supposition, an increase in the number of V_A , which is acceptors, will enhance resistivity or decrease σ . This can be explained on the fact that, in n-type material, electrons will be available in the conduction band. With increasing number of vacancies (i.e., acceptors), electrons will be captured by these vacancies and hence reducing the electrons in conduction band, and this results a decrease in conductivity. The high V_A concentration in the specimens results σ minimal. Chemical analysis of $\text{Na}_{1-x}\text{K}_x\text{TaO}_3$ samples shows significant deficiency of Na, which supports the observed conductivity behavior of these compositions. Similar results were obtained by Raevskii et al. [15] for $\text{Na}_{1-x}\text{K}_x\text{NbO}_3$ system.

Wrobel et al. [16] have reported the results on the electrical properties ordinarily sintered Zr-Ti-Pb ceramics. All the specimens investigated had p-type conductivity. The concentration dependence of σ exhibited a distinct maximum corresponding to certain concentrations. These results agree closely with the above given assumptions, because in the case of hole conductivity, an increase in V_A concentration, must increase σ .

Dielectric conductivity is greatly influenced by porosity, and decreases as the porosity increases, in proportion for small values of porosity corresponding to isometric uniformly distributed pores, such as are normally present. For large amount of porosity the effect of pores is more substantial.

Oxygen vacancies could exist in a perfect system, which contribute dominantly in dielectric conductivity mechanism [17-20]. The role of the oxygen vacancies consists in its ability to bind one or two electrons creating F_1 and F_2 centres. Empty vacancies and mono-electron states can be considered as the deep and shallow trap states or acceptor states. The F_2 states, which are able to give one electron to the conduction band, can be treated as donors. Therefore, the oxide system, having deficiency of metal or deficiency of oxygen, can show properties of the p-type or n-type semiconductor, respectively [21]. In $\text{Na}_{1-x}\text{K}_x\text{TaO}_3$, an essential role is played not only by the presence of oxygen defects but also by their polarization produced by the polarizing field applied or by the measuring field. The effective polarization during the action of the field is composed of inertialess induced polarization, the inertial polarization of the space charge and the spontaneous polarization (for the ferroelectric state). The effective polarization determines the processes of charge exchange with the electrodes. It also determines the effective current in the sample circuit. The injected electrons can cause the transition of empty oxygen vacancies and F_1 states localized inside the near-electrode layer to F_2 states. At sufficient high temperature the thermal generation of electrons forms F_2 centres and the subsequent transition to the F_1 state can take place, consequently, some coupling takes place. The polarization of the ion space charge stimulates the process of injection of carriers from the electrodes; the injected charges screen this polarization thus producing its unusual stability and behavior, which is similar to the electret effect.

REFERENCES

- [1]. G. A. Samara, *Ferroelectrics*, Vol. 73, 145, 1987.
- [2]. G. A. Samara and P. S. Peercy, *Solid State Physics*, (ed) H. Ehrenreich, F. Seitz and D. Turnbull, New York: Academic Press, 1981.
- [3]. T. G. Davis, *Phys. Rev.*, Vol. B5, 2530, 1972.
- [4]. G. A. Samara, *Proc. of the 6th International Meeting on Ferroelectricity*, Kobe, Japan, 1985.
- [5]. P. Vousden, *Acta Cryst.*, Vol. 4, 373, 1951.
- [6]. B. D. Cullity, *Elements of X-ray Diffraction*, Addison-Wesley Publishing Company Inc., 1977.
- [7]. L. V. Azaroff, *Elements of X-ray Crystallography*, New York: McGraw Hill Book Company, 1968.
- [8]. H. F. Kay and J. L. Miles, *Acta Cryst.*, Vol. 10, 213, 1957.
- [9]. F. Jona and G. Shirane, *Ferroelectric Crystals*, Pergamon Press, 1962.
- [10]. A. Reisman and E. Banks, *J. Amer. Ceram. Soc.*, Vol. 80, 1877, 1958.
- [11]. G. Goodman, R. C. Buchanan and T. G. Reynolds, *Ceramic Materials for Electronics; Processing, Properties, and Application*, (ed) R. C. Buchanan, New York: Marcel Dekker Inc., 1991.
- [12]. B. Jaffe, W. Cook and H. Jaffe, *Piezoelectric Ceramics*, Moscow: Mir Publishers, 1974.

- [13]. J. Tanaka, M. Tsukioka, Y. Miyazawa, Y. Mori and S. Shimazu, Solid State Comm., Vol. 34, 221, 1980.
- [14]. H. Handerek and M. Badurski, Pr. Nauk. U. S1. Katowicach, Vol. 127, 107, 1976.
- [15]. I. P. Raevskii, L. A. Reznichenko, O. I. Prokopalo and E. G. Fesenko, Izv. Akad. Nauk. SSSR, Neorg. Mater., Vol. 15, 872, 1979.
- [16]. Z. Wrobel and J. Handerek, Pr. Nauk. U. S1. Katowicach, Vol. 127, 175, 1976.
- [17]. O. I. Prokopalo, Izv. Akad. Nauk. SSSR, Vol. 29, 1009, 1965.
- [18]. J. Handerek and Z. Ujma, Postepy Fizyki, Vol. 29, 25, 1978.
- [19]. J. Handerek, A. Aleksandrowicz and M. Badurski, Acta Physica Polonica, Vol. A56, 769, 1979.
- [20]. E. V. Bursyan, Nonlinear crystal-Barium Titanate, Moskva : Nauka Press, 1974.
- [21]. V. A. Bokov and I. E. Myl'nikova, Sov. Phys. Solid state, Vol. 3, 613, 1961.